

Short communication

Electrochemical stability of core–shell structure electrode for high voltage cycling as positive electrode for lithium ion batteries

B.-C. Park^a, H.J. Bang^a, K. Amine^b, E. Jung^c, Y.-K. Sun^{a,*}

^a Department of Chemical Engineering, Hanyang University, Seoul 133-791, South Korea

^b Electrochemical Technology Program, Chemical Engineering Division, Argonne National Laboratory, Argonne, IL 60493, USA

^c Department of Digital Culture & Contents, Dong-Eui University, Busan 614-714, South Korea

Available online 27 June 2007

Abstract

The core–shell type cathode material $\text{Li}[(\text{Ni}_{0.8}\text{Co}_{0.1}\text{Mn}_{0.1})_{0.8}(\text{Ni}_{0.5}\text{Mn}_{0.5})_{0.2}]\text{O}_2$ (CS) for Li-ion battery was synthesized via co-precipitation method. The electrochemical and thermal properties of the core–shell structured $\text{Li}[(\text{Ni}_{0.8}\text{Co}_{0.1}\text{Mn}_{0.1})_{0.8}(\text{Ni}_{0.5}\text{Mn}_{0.5})_{0.2}]\text{O}_2$ were compared with those of the average composition of core–shell $\text{Li}[\text{Ni}_{0.74}\text{Co}_{0.08}\text{Mn}_{0.18}]\text{O}_2$ (ACCS) and the mixture of the core $\text{Li}[\text{Ni}_{0.8}\text{Co}_{0.1}\text{Mn}_{0.1}]\text{O}_2$ and the shell $\text{Li}[\text{Ni}_{0.5}\text{Mn}_{0.5}]\text{O}_2$ material (MCS). The CS shows the enhanced electrochemical properties in a high voltage range (4.5 V and 4.6 V) as well as the typical cut-off voltage range (4.3 V). The capacity retentions of CS, core, and ACCS material were 94.2% (176.9 mAh g⁻¹), 86.6% (172 mAh g⁻¹), and 88.4% (169.3 mAh g⁻¹) after 120 cycles, respectively.

© 2007 Elsevier B.V. All rights reserved.

Keywords: Core–shell; Co-precipitation; Cathode; Lithium ion battery

1. Introduction

Extensive research effort has been focusing on finding new positive electrodes for Li-ion Batteries. Due to high cost of LiCoO_2 , currently used as a cathode material in commercial lithium battery system, extensive effort has been made to develop cheaper cathode materials with better electrochemical performance than LiCoO_2 . The layered materials such as $\text{Li}[\text{Ni}_{0.8}\text{Co}_{0.2}]\text{O}_2$ [1], $\text{Li}[\text{Ni}_{0.5}\text{Mn}_{0.5}]\text{O}_2$ [2], and $\text{Li}[\text{Ni}_{1/3}\text{Co}_{1/3}\text{Mn}_{1/3}]\text{O}_2$ [3] are candidates as promising cathode materials. However, all candidate materials have technical issues for application on Li-ion battery system.

Recently, the micro-scale core–shell structured $\text{Li}[(\text{Ni}_{0.8}\text{Co}_{0.1}\text{Mn}_{0.1})_{0.8}(\text{Ni}_{0.5}\text{Mn}_{0.5})_{0.2}]\text{O}_2$ has been introduced in our previous paper [4,5]. This material shows a synergetic effect with good points of two materials. The one is a higher capacity for $\text{Li}[\text{Ni}_{0.8}\text{Co}_{0.1}\text{Mn}_{0.1}]\text{O}_2$ as the core, the other is a good thermal stability for $\text{Li}[\text{Ni}_{0.5}\text{Mn}_{0.5}]\text{O}_2$ as the shell.

In this study, we investigate electrochemical performance and stability of the core–shell structured $\text{Li}[(\text{Ni}_{0.8}\text{Co}_{0.1}\text{Mn}_{0.1})_{0.8}$

$(\text{Ni}_{0.5}\text{Mn}_{0.5})_{0.2}]\text{O}_2$ (hereafter refer to CS) in high voltage range (4.5 V and 4.6 V) in comparison with mechanically blend of core material and shell material ($\text{Li}[\text{Ni}_{0.8}\text{Co}_{0.1}\text{Mn}_{0.1}]\text{O}_2$: $\text{Li}[\text{Ni}_{0.5}\text{Mn}_{0.5}]\text{O}_2$ = 8:2, hereafter refer to MCS). In addition, the cathode material that has an average chemical composition of core–shell ($\text{Li}[\text{Ni}_{0.74}\text{Co}_{0.08}\text{Mn}_{0.18}]\text{O}_2$, hereafter refer to ACCS) was synthesized and compared with electrochemical properties of CS material.

2. Experimental

The $[(\text{Ni}_{0.8}\text{Co}_{0.1}\text{Mn}_{0.1})_{0.8}(\text{Ni}_{0.5}\text{Mn}_{0.5})_{0.2}](\text{OH})_2$ and $[\text{Ni}_{0.74}\text{Co}_{0.08}\text{Mn}_{0.18}](\text{OH})_2$ compounds were synthesized by a co-precipitation method [4]. Also, the core $[\text{Ni}_{0.8}\text{Co}_{0.1}\text{Mn}_{0.1}](\text{OH})_2$ and the shell $[\text{Ni}_{0.5}\text{Mn}_{0.5}](\text{OH})_2$ materials were synthesized using same method. An aqueous solution of $\text{NiSO}_4 \cdot 6\text{H}_2\text{O}$, $\text{CoSO}_4 \cdot 7\text{H}_2\text{O}$ and $\text{MnSO}_4 \cdot 5\text{H}_2\text{O}$ was pumped into a continuously stirred tank reactor under N_2 purging. Simultaneously, a NaOH solution(aq) and an appropriate amount of NH_4OH solution(aq) as a chelating agent were fed separately into the reactor. During the co-precipitation reaction, initially formed particles grew into spherical particles through vigorous stirring.

In order to construct the core–shell material for the composition of $[(\text{Ni}_{0.8}\text{Co}_{0.1}\text{Mn}_{0.1})_{0.8}(\text{Ni}_{0.5}\text{Mn}_{0.5})_{0.2}](\text{OH})_2$, the

* Corresponding author. Tel.: +82 2 2220 0524; fax: +82 2 2282 7329.
E-mail address: yksun@hanyang.ac.kr (Y.-K. Sun).

obtained $[\text{Ni}_{0.8}\text{Co}_{0.1}\text{Mn}_{0.1}](\text{OH})_2$ was continuously mixed with the solution containing metal compounds (cationic ratio of Ni:Mn = 1:1) in the reactor. The final precursor was dried at 120 °C for 12 h to remove adsorbed water. The dried precursor was mixed with a stoichiometric amount of $\text{LiOH}\cdot\text{H}_2\text{O}$ and heated at 770 °C for 20 h.

Powder X-ray diffraction (Rigaku, Rint-2000) using Cu K α radiation was used to identify crystalline phase of the final products. The morphology of the prepared powders was also observed using scanning electron microscopy (SEM, JSM-6340F, JEOL).

Chemical compositions of the prepared powder were analyzed with an atomic absorption spectroscopy (Vario 6, Analyticjena).

Electrochemical performance of the prepared powder was evaluated with coin type cell (CR2032). The cell consisted of the positive and the lithium metal negative electrodes separated by porous polypropylene film. The positive electrode was fabricated with the mixture of the prepared powder and conducting binder (mixture of teflonized acetylene black (TAB) and graphite). Electrolyte solution was 1 M LiPF_6 in a mixture of ethylene carbonate (EC) and diethyl carbonate (DEC) in a 1:1 volume ratio (Cheil Industries Inc., Korea). For differential scanning calorimetry (DSC) experiments, the cells were finally fully charged to 4.3 V and opened in the Ar-filled dry box. The remaining excess electrolyte on the electrode was removed and was inserted into the gold plated stainless steel sample pan. The thermal scan was performed in DSC (NETZSCH 200PC Germany) at scan rate of 10 °C min^{-1} from 50 °C to 400 °C.

3. Results and discussion

The Fig. 1 shows the cross-sectional SEM images of the synthesized ACCS ($\text{Li}[\text{Ni}_{0.74}\text{Co}_{0.08}\text{Mn}_{0.18}]\text{O}_2$) and CS ($\text{Li}[(\text{Ni}_{0.8}\text{Co}_{0.1}\text{Mn}_{0.1})_{0.8}(\text{Ni}_{0.5}\text{Mn}_{0.5})_{0.2}]\text{O}_2$) powders. As seen from Fig. 1(a), the $\text{Li}[\text{Ni}_{0.74}\text{Co}_{0.08}\text{Mn}_{0.18}]\text{O}_2$ particle has a spherical shape with the average particle size of approximately 12 μm in a diameter. The SEM image of the $\text{Li}[(\text{Ni}_{0.8}\text{Co}_{0.1}\text{Mn}_{0.1})_{0.8}(\text{Ni}_{0.5}\text{Mn}_{0.5})_{0.2}]\text{O}_2$ shows the clear existence of the shell type structure which was uniformly covering the core material with 1 μm thickness.

In order to determine the chemical composition of the prepared cathode material, AAS (atomic absorption spectroscopy) analysis was carried out and the result was summarized in Table 1. AAS result shows that the chemical composition of the CS has almost same composition of the ACCS.

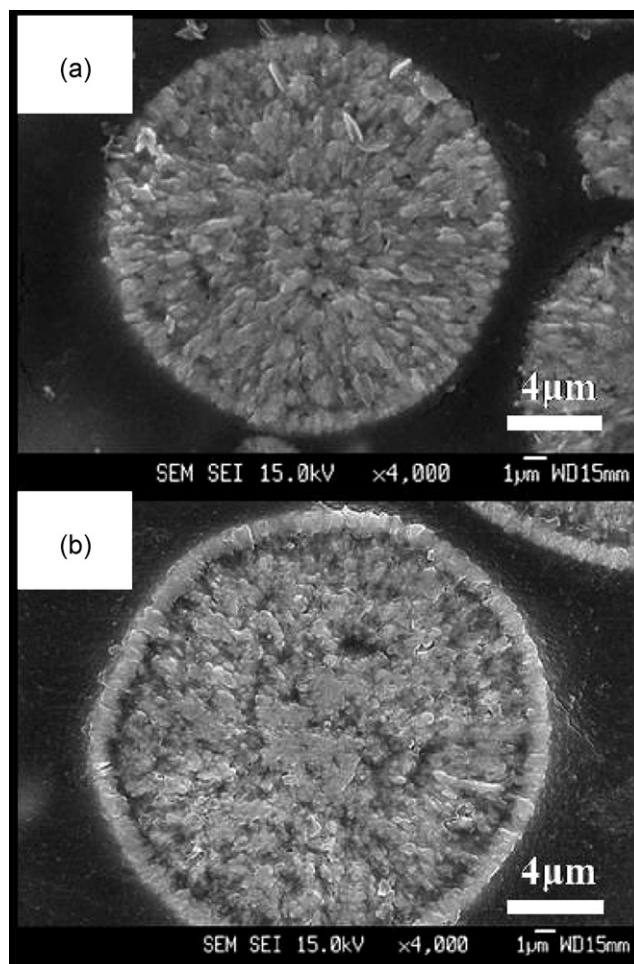


Fig. 1. Cross-sectional SEM images of (a) ACCS ($\text{Li}[\text{Ni}_{0.74}\text{Co}_{0.08}\text{Mn}_{0.18}]\text{O}_2$) and (b) CS ($\text{Li}[(\text{Ni}_{0.8}\text{Co}_{0.1}\text{Mn}_{0.1})_{0.8}(\text{Ni}_{0.5}\text{Mn}_{0.5})_{0.2}]\text{O}_2$).

The XRD patterns of core, CS, and ACCS are shown in Fig. 2. All the powders were confirmed to have a well-defined hexagonal $\alpha\text{-NaFeO}_2$ structure with space group $R\bar{3}m$. No impurity peaks were observed from the XRD patterns.

The initial charge and discharge curves of the core, CS, MCS and ACCS materials are shown in Fig. 3. The cells were cycled at a constant current density of 20 mA g^{-1} in the voltage range of 3.0–4.3 V. The core, ACCS, and CS electrode initially delivered the similar specific capacity of 200 mAh g^{-1} , 195 mAh g^{-1} , and 188 mAh g^{-1} , respectively. It seems that the encapsulation of the core material $\text{Li}[\text{Ni}_{0.8}\text{Co}_{0.1}\text{Mn}_{0.1}]\text{O}_2$ with the shell material $\text{Li}[\text{Ni}_{0.5}\text{Mn}_{0.5}]\text{O}_2$ did not significantly hinder the electrochemical properties of the core material. The charge curve of the

Table 1

Chemical composition of the prepared powders determined by AAS

	Chemical composition as prepared	Chemical composition determined by AAS result
Core	$\text{Li}[\text{Ni}_{0.8}\text{Co}_{0.1}\text{Mn}_{0.1}]\text{O}_2$	$\text{Li}[\text{Ni}_{0.8}\text{Co}_{0.101}\text{Mn}_{0.09}]\text{O}_2$
CS	$\text{Li}[(\text{Ni}_{0.8}\text{Co}_{0.1}\text{Mn}_{0.1})_{0.8}(\text{Ni}_{0.5}\text{Mn}_{0.5})_{0.2}]\text{O}_2$	$\text{Li}[\text{Ni}_{0.739}\text{Co}_{0.08}\text{Mn}_{0.181}]\text{O}_2$
ACCS	$\text{Li}[\text{Ni}_{0.74}\text{Co}_{0.08}\text{Mn}_{0.18}]\text{O}_2^a$	$\text{Li}[\text{Ni}_{0.74}\text{Co}_{0.08}\text{Mn}_{0.18}]\text{O}_2$
Shell	$\text{Li}[\text{Ni}_{0.5}\text{Mn}_{0.5}]\text{O}_2$	$\text{Li}[\text{Ni}_{0.502}\text{Mn}_{0.498}]\text{O}_2$

^a Average composition of the CS.

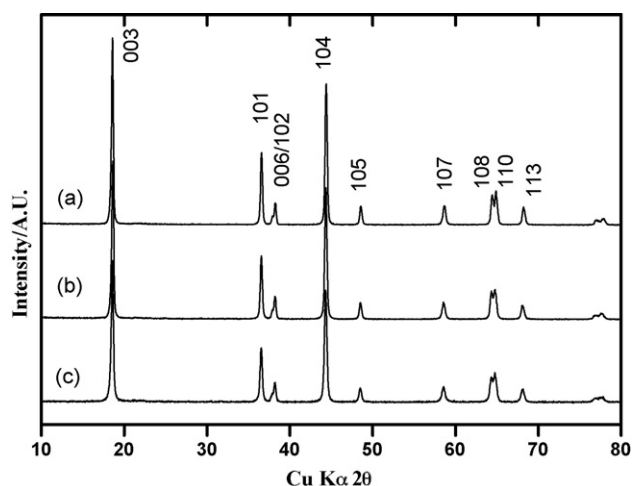


Fig. 2. XRD patterns of the prepared (a) core ($\text{Li}[\text{Ni}_{0.8}\text{Co}_{0.1}\text{Mn}_{0.1}]\text{O}_2$), (b) CS ($\text{Li}[(\text{Ni}_{0.8}\text{Co}_{0.1}\text{Mn}_{0.1})_{0.8}(\text{Ni}_{0.5}\text{Mn}_{0.5})_{0.2}]\text{O}_2$) and (c) ACCS ($\text{Li}[\text{Ni}_{0.74}\text{Co}_{0.08}\text{Mn}_{0.18}]\text{O}_2$).

CS electrode show higher than that of core electrode, which is ascribed to the existence of shell layer on the core. Geometrically, the shell composition locates the outer-layer of the core material. Reversible lithium extraction/insertion during cycling may occur preferentially in the shell material. The curve of CS electrode might be influenced by the electrochemical properties of the shell material. It has been known that $\text{Li}[\text{Ni}_{0.5}\text{Mn}_{0.5}]\text{O}_2$ (shell) material exhibits relatively higher electric resistance than that of the $\text{Li}[\text{Ni}_{0.8}\text{Co}_{0.1}\text{Mn}_{0.1}]\text{O}_2$ (core) [6]. It can be seen from Fig. 3 that the MCS delivers quite lower discharge capacity of 160 mAh g^{-1} than that of core-shell type material.

The comparison of cycling performance for the prepared core, ACCS, CS, and MCS material was shown in Fig. 4. The cells were cycled at a constant current of 20 mA g^{-1} in the voltage range of 3.0–4.3 V. The capacity loss of the CS material is milder than those of core and ACCS material over 120 cycles. The capacity retention of CS material is about 94.2% after 120

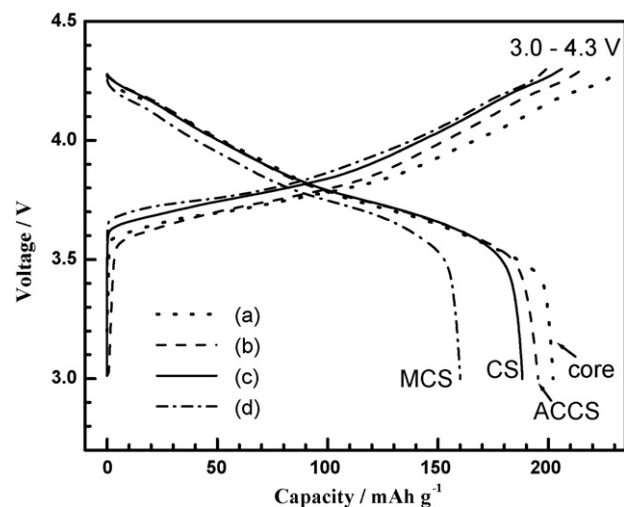


Fig. 3. Comparison of the initial charge–discharge curves of (a) core, (b) ACCS (c) CS and (d) MCS in the voltage range of 3.0–4.3 V at current level of 20 mA g^{-1} (C/10).

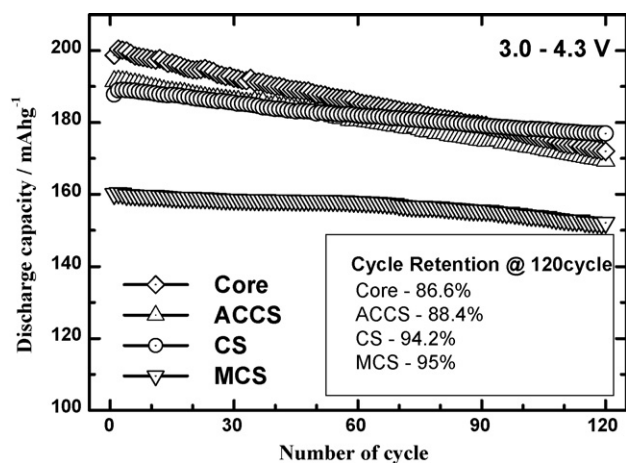


Fig. 4. Discharge capacity vs. cycle no. of core, ACCS, CS and MCS cells cycled at a current density of 20 mA g^{-1} (C/10) in the voltage range of 3.0–4.3 V.

cycles (86.6% and 88.4% for core and ACCS material, respectively). ACCS electrode showed also better capacity retention than that of core material due to lower Ni content. However, after 100 cycle, the capacity fade of ACCS became similar to that

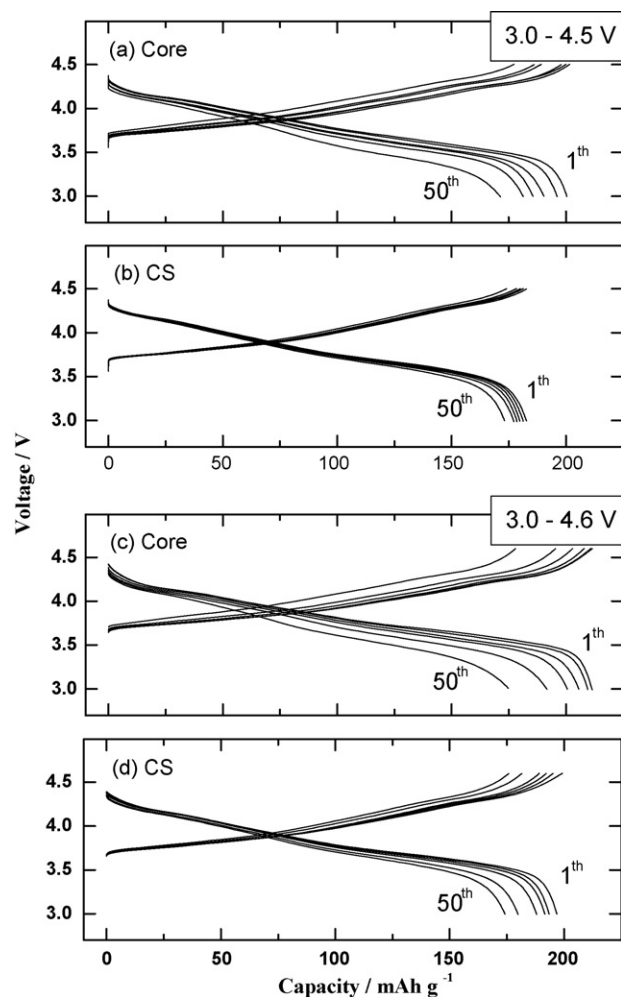


Fig. 5. Comparison of cycling performance of core and CS in the voltage range of 4.5 V for (a) and (b) and 4.6 V for (c) and (d) at current level of 100 mA g^{-1} (C/2).

of core material. MCS cell showed a stable cycle performance compared with the other cells, but after 90 cycle, the capacity fading rate increased. The improved cyclability of the CS material probably results from the existence of the shell material. The $\text{Li}[\text{Ni}_{0.5}\text{Mn}_{0.5}]\text{O}_2$ (shell) is known to have a stable cycling performance due to its structural stability [2]. It has been previously reported that LiNiO_2 and its derivatives $\text{Li}[\text{Ni}_{1-x}\text{Co}_x]\text{O}_2$ suffer from the structural instability caused by structural deformation especially when cycled above 4.3 V. Furthermore, Co dissolution induced by HF generated from the electrolyte in the presence of H_2O deteriorates the $\text{Li}[\text{Ni}_{1-x}\text{Co}_x]\text{O}_2$ type material. The core material $\text{Li}[\text{Ni}_{0.8}\text{Co}_{0.1}\text{Mn}_{0.1}]\text{O}_2$ surround by structurally stable $\text{Li}[\text{Ni}_{0.5}\text{Mn}_{0.5}]\text{O}_2$ might be protected from the reaction between electrolyte and the surface of the particles.

In order to evaluate the electrochemical stability of CS material for high voltage range cycling, core and CS electrode were cycled in the voltage range of 4.5 V and 4.6 V measured using a constant current of 100 mA g^{-1} . Fig. 5 shows the cycling performance of core and CS for different voltage ranges (4.5 V and 4.6 V). Core electrode cycled in the voltage of 3.0–4.5 V delivered an initial discharge capacity of 199 mAh g^{-1} with gradual decrease of discharge capacity as shown in Fig. 5(a). At 50th cycle, the capacity retention of core is 85.9% (171 mAh g^{-1}). Although CS electrode initially delivered a lower capacity of

183 mAh g^{-1} , the capacity retention of the electrode reach to 93.4% after 50 cycles which is similar capacity of core (191 mAh g^{-1}). The capacity retentions of core and CS cells in the voltage range of 3.0–4.6 V are analogous to the result observed from 4.5 V cut-off cycling as shown in Fig. 5(c) and (d). The capacity retention of core and CS cycled for cut-off voltage of 4.6 V are 83.8% and 88.3%, respectively.

The thermal stability of the core, ACCS, core–shell (CS), MCS and shell material was evaluated by using DSC (differential scanning calorimetry). The core ($\text{Li}_{1-x}[\text{Ni}_{0.8}\text{Co}_{0.1}\text{Mn}_{0.1}]\text{O}_2$) showed a large exothermic peak at 217°C with an onset of decomposition near 190°C , and the reaction released 3285 J g^{-1} of heat. The ACCS materials showed an enhanced thermal stability due to lower Ni content but it had a larger heat generation of 3458 J g^{-1} . On the other hand, the shell $\text{Li}_{1-x}[\text{Ni}_{0.5}\text{Mn}_{0.5}]\text{O}_2$ is stable up to 285°C , which is well accordance with the previous report [6]. Meanwhile, the thermal stability of CS ($\text{Li}_{1-x}[(\text{Ni}_{0.8}\text{Co}_{0.1}\text{Mn}_{0.1})_{0.8}(\text{Ni}_{0.5}\text{Mn}_{0.5})_{0.2}]\text{O}_2$) was greatly improved compared with core. Its generated heat of 2261 J g^{-1} exhibits a relatively small with an onset temperature at 205°C . The improved thermal stability of the CS ($\text{Li}_{1-x}[(\text{Ni}_{0.8}\text{Co}_{0.2})_{0.8}(\text{Ni}_{0.5}\text{Mn}_{0.5})_{0.2}]\text{O}_2$) could be ascribed to the thermally stable outer $\text{Li}[\text{Ni}_{0.5}\text{Mn}_{0.5}]\text{O}_2$ shell [4], which would suppress the oxygen release from the host lattice. Another reason for the improved thermal stability of CS material would be that the thermally stable outer $\text{Li}[\text{Ni}_{0.5}\text{Mn}_{0.5}]\text{O}_2$ shell tightly encapsulated the core material so that the thermally instable $\text{Li}_{1-x}[\text{Ni}_{0.8}\text{Co}_{0.1}\text{Mn}_{0.1}]\text{O}_2$ core did not directly contact with electrolyte solution. The complex thermal behavior combined characteristics of core and shell materials was observed for MCS which the exothermic reaction starts from 180°C continuing to 300°C (Fig. 6).

4. Conclusion

The core–shell structure cathode material $\text{Li}[(\text{Ni}_{0.8}\text{Co}_{0.1}\text{Mn}_{0.1})_{0.8}(\text{Ni}_{0.5}\text{Mn}_{0.5})_{0.2}]\text{O}_2$ was synthesized by co-precipitation method. In order to confirm the synergetic effect of core–shell structure, MCS and ACCS were also prepared. MCS cell delivered lower discharge capacity, compared to those of core, CS and ACCS cell. Also ACCS with same average chemical composition of CS initially delivered similar discharge capacity to the core material but the capacity retention is not improved as good as CS material. The outer layer of core–shell material consist of the electrochemical and thermally stable $\text{Li}[\text{Ni}_{0.5}\text{Mn}_{0.5}]\text{O}_2$. The thickness of shell was approximately $1 \mu\text{m}$ estimated by SEM. The existence of the electrochemically stable shell on the surface of core played as a protecting layer and improved the cycling performance of the core as well as thermal stability.

Acknowledgement

This work was supported by University IT Research Center Project.

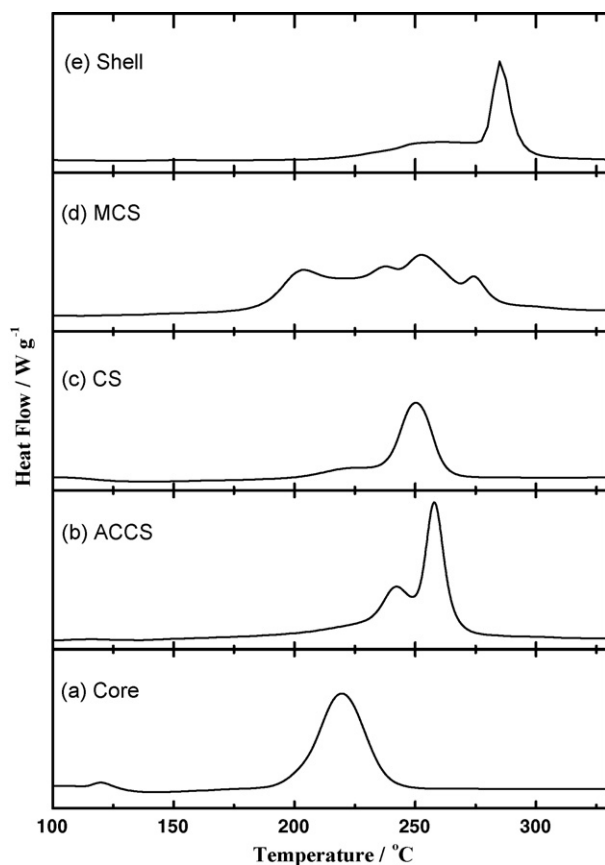


Fig. 6. Differential scanning calorimetry (DSC) traces of core, ACCS, core–shell (CS), MCS and shell. (a) Core, (b) ACCS, (c) CS, (d) MCS and (e) shell. Scan rate = $10^\circ\text{C min}^{-1}$.

References

- [1] M.-H. Kim, H.-S. Shin, D.W. Shin, Y.-K. Sun, *J. Power Sources* 159 (2006) 1328.
- [2] Y.-K. Sun, S.-H. Kang, K. Amine, *Mater. Res. Bull.* 39 (2004) 819.
- [3] G.-H. Kim, J.-H. Kim, C.-S. Yoon, Y.-K. Sun, *J. Electrochem. Soc.* 152 (2005) A1707.
- [4] Y.-K. Sun, S.-T. Myung, M.-H. Kim, J. Prakash, K. Amine, *J. Am. Chem. Soc.* 127 (2005) 13411.
- [5] Y.-K. Sun, S.-T. Myung, M.-H. Kim, J.-H. Kim, *Electrochem. Solid-State Lett.* 9 (2006) A171.
- [6] S.-H. Kang, J. Kim, M.E. Stoll, D. Abraham, Y.-K. Sun, K. Amine, *J. Power Sources* 112 (2002) 41.